

*Letter to the Editor***Low-mass stars in the massive H II region NGC 3603*****Deep NIR imaging with ANTU/ISAAC****B. Brandl¹, W. Brandner², F. Eisenhauer³, A.F.J. Moffat⁴, F. Palla⁵, and H. Zinnecker⁶**¹ Cornell University, Department of Astronomy, 222 Space Sciences Building, Ithaca, NY 14853, USA (brandl@astrosun.tn.cornell.edu)² University of Hawaii, Institute for Astronomy, 2680 Woodlawn Dr., Honolulu, HI 96822, USA³ Max-Planck-Institut für Extraterrestrische Physik, Giessenbachstrasse, 85740 Garching, Germany⁴ Université de Montréal, Département de physique, C.P. 6128, Succ. Centre-ville, Montréal, QC, H3C 3J7, Canada and Observatoire du mont Mégantic⁵ Osservatorio Astrofisico di Arcetri, Largo E.Fermi 5, 50125 Firenze, Italy⁶ Astrophysikalisches Institut Potsdam, An der Sternwarte 16, 14482 Potsdam, Germany

Received 8 September 1999 / Accepted 11 October 1999

Abstract. We have observed NGC 3603, the most massive visible H II region known in the Galaxy, with ANTU(VLT1)/ISAAC in the near-infrared (NIR) J_s , H , and K_s -bands. Our observations are the most sensitive observations made to date of this dense starburst region, allowing us to investigate with unprecedented quality its low-mass stellar population. Our mass limit to stars detected in all three bands is $0.1M_\odot$ for a pre-main sequence star of age 0.7 Myr. The overall age of the pre-main sequence stars in the core region of NGC 3603 has been derived from isochrone fitting in the colour-magnitude diagram, leading to 0.3–1.0 Myr. The NIR luminosity functions show that the cluster is populated in low-mass stars at least down to $0.1M_\odot$. Our observations clearly show that sub-solar mass stars do form in massive starbursts.

Key words: telescopes – stars: Hertzsprung–Russel (HR) and C-M diagrams – stars: pre-main sequence – ISM: H II regions – galaxies: starburst

1. Introduction

NGC 3603 is located in the Carina spiral arm (RA = 11^h , DEC = -61°) at a distance of $\sim 6 - 7$ kpc (De Pree et al. 1999, and references therein). It is the only massive, Galactic H II region whose ionizing central cluster can be studied at optical wavelengths due to only moderate (mainly foreground) extinction of $A_V \approx 4.5^m$ (Eisenhauer et al. 1998). The OB stars ($\geq 10M_\odot$) contribute more than $2000M_\odot$ to the cluster mass. In comparison to the Orion Trapezium system, NGC 3603 with its more than 50 O and WR stars (Moffat, Drissen & Shara

1994) producing a Lyman continuum flux of $10^{51}s^{-1}$ (Kennicutt 1984; Drissen et al. 1995) has about 100 times the ionizing power of the Trapezium cluster. With a bolometric luminosity $L_{bol} > 10^7 L_\odot$, NGC 3603 has about 10% of the luminosity of 30 Doradus and looks in many respects very similar to its stellar core R136 (Brandl et al. 1996). In fact it has been called a Galactic clone of R136 without the massive surrounding cluster halo (Moffat, Drissen & Shara 1994). In many ways NGC 3603 and R136 can be regarded as representative building blocks of more distant and luminous starburst galaxies (Brandl, Brandner & Zinnecker 1999, and references therein).

Although NGC 3603 has been the target of many recent ground and space based studies (Eisenhauer et al. 1998; Brandner et al. 2000) little is known about its content of sub-solar mass stars. Our general aim is to investigate low-mass star formation in the violent environments of starburst regions (Brandl, Brandner & Zinnecker 1999). Several fundamental questions arise in this context: Does the slope of the IMF vary on small scales? Do low-mass stars in a starburst event form together with the most massive stars or do they form at different times or on different timescales? And finally, one might even ask if low-mass stars form at all in such environments.

2. Observations and data reduction

NGC 3603 was observed in the $J_s = 1.16\text{--}1.32\ \mu\text{m}$, $H = 1.50\text{--}1.80\ \mu\text{m}$, and $K_s = 2.03\text{--}2.30\ \mu\text{m}$ broadband filters using the NIR camera ISAAC mounted on ANTU, ESO's first VLT. The observations were made during the 4 nights of April 4–6 and 9, 1999, in service mode when the optical seeing was equal or better than $0''.4$ on Paranal. Such seeing was essential for accurate photometry in the crowded cluster and increased our sensitivity to the faintest stars. The majority of our data were taken under photometric conditions.

Send offprint requests to: B. Brandl

* Based on observations obtained at the European Southern Observatory, Paranal (ESO Proposal ID 63.I-0015)



Fig. 1. Three colour image of NGC 3603 composed from J_s (blue), H (green), and K_s -band (red) images. Intensities are scaled in logarithmic units; FOV is $3\frac{1}{4} \times 3\frac{1}{4}$ (6.2×6.2 parsec²). North is up, East to the left. The insert to the lower right is a blow up of the central parsec².

Our observing strategy was to use the shortest possible frame times (1.77s) to keep the number of saturated stars to a minimum. However, due to the system’s excellent sensitivity, about two dozen of the brightest stars ended up being saturated. Nevertheless, this does not impose a problem to our study of the low mass stars. Thirty-four short exposures were co-added to an effective one-minute exposure, the minimum time per pointing required to stabilize the telescope’s active optics control system. Between the 1 minute pointings we moved the telescope

by up to $20''$ offsets in a random pattern. This approach has several advantages:

- Enlargement of the observed field of view (FOV) with maximum signal-to-noise (S/N) in the cluster center.
- Reduction of residual images and other array artefacts, using the median filtering technique.
- Derivation of the “sky” from the target exposures using the median filtering technique. No additional time for “blank” sky frames outside the cluster was required.

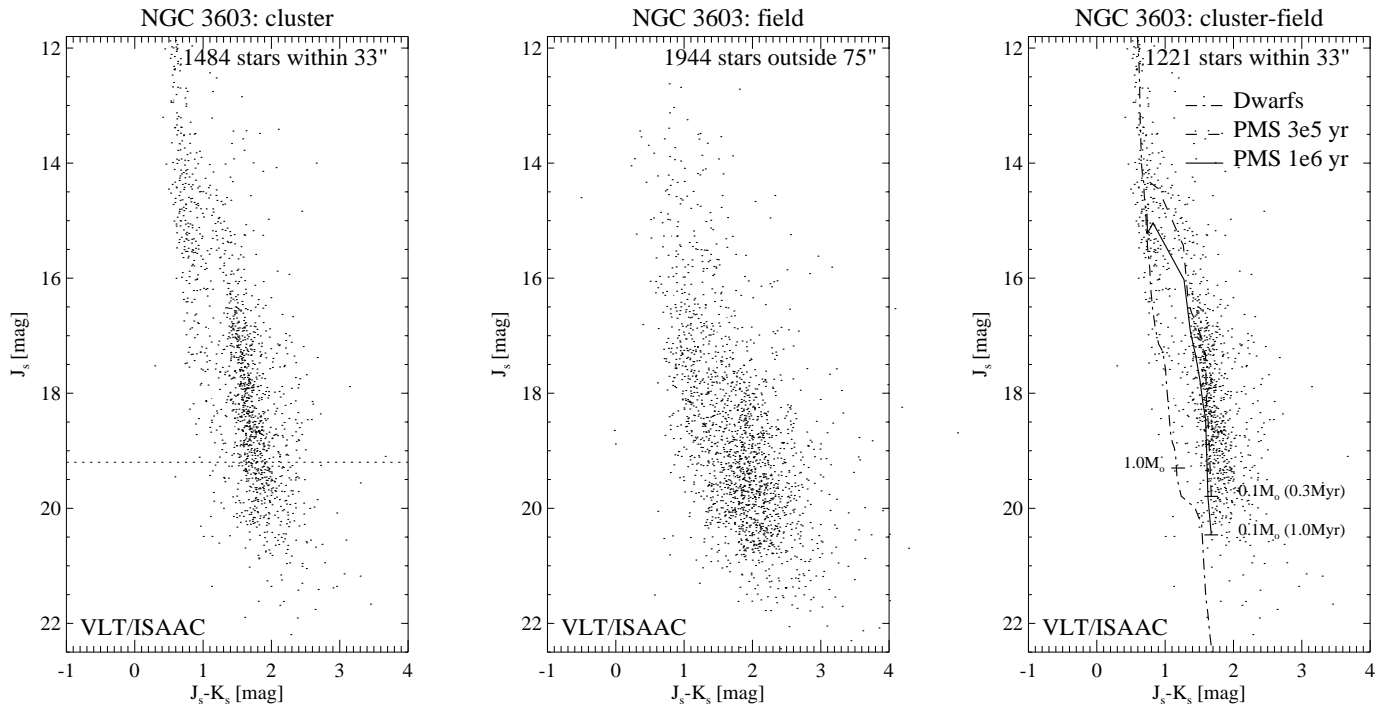


Fig. 2a–c. J_s versus $J_s - K_s$ colour-magnitude diagrams of NGC 3603. **a** contains all stars detected in all three wavebands within the central $r \leq 33''$ (1 pc) [$1''^2$], **b** shows the field stars at $r \geq 75''$ (2.25 pc) [$6.3''^2$] around the cluster, and **c** shows the cluster population within $r \leq 33''$ with the field stars statistically subtracted. The dashed horizontal line indicates the detection limit of the previous most sensitive NIR study by Eisenhauer et al. (1998). **c** also shows the theoretical isochrones of pre-main sequence stars of different ages from Palla & Stahler (1999) and the main sequence for dwarfs. For comparison we’ve plotted some corresponding stellar masses next to the isochrones.

The sky frames have been computed using between 15 and 37 subsequent exposures per waveband and night, and careful eye-inspection showed that all sources have been efficiently removed using our modified median filtering technique which returns the lower 1/3 instead of the mean (1/2) value. We subtracted the sky-background and flat-fielded each exposure using the twilight flat-fields provided by ESO. The relative position offsets were derived from cross-correlating the images; the exposures were co-aligned on a 0.5×0.5 -pixel subgrid for better spatial resolution, and then added together using the median filtering technique. The resulting images are 3.4×3.4 in size with pixels of $0.''074$. The effective exposure times of the final broadband images in the central 2.5×2.5 is 37, 45, and 48 minutes in J_s , H , and K_s , respectively. Fig. 1 shows the impressive 3-colour composite image. The brightest star in the FOV ($80''$ north-east of the core) is the red supergiant IRS 4 (Frogel, Persson, & Aaronson 1977). The ring nebula and the bipolar outflows around the blue supergiant Sher 25 (Brandner et al. 1997) about $18''$ north of the core are clearly detected in the K band. The image also shows the three proplyd-like objects that have been recently discovered by Brandner et al. (2000); these proplyds are similar to those seen in Orion but about 20–30 times more extended. About $1'$ south of the central cluster, we detect the brightest members of the deeply embedded proto cluster IRS 9.

In order to derive the photometric fluxes of the stars we used the IRAF implementation of DAOPHOT (Stetson 1987). We first ran DAOFIND to detect the individual sources, leading

to $\sim 20,000$ peaks in each waveband. Many of these may be noise or peaks in the nebular background and appear only in one waveband. In order to reject spurious sources, we required that sources be detected independently in all three wavebands, and that the maximal deviation of the source position centroid between different wavebands be less than $0.075''$. The resulting source list contains 6967 objects in the entire FOV.

We then flux-calibrated the images using the faint NIR standard stars from the lists by Hunt et al. (1998) and Persson et al. (1998). Because of the stringent requirements on the seeing the PSF did not noticeably change during our observations and the systematic photometric errors are dominated by uncertainties in the aperture offsets. (A detailed error analysis will be part of a subsequent paper). Comparing our photometric fluxes of numerous sources with the fluxes derived by Eisenhauer et al. (1998) yields a systematic offset of 0.1^m in J_s and 0.05^m in K_s .

3. Results and interpretation

Fig. 2a–c shows the resulting colour-magnitude diagrams (CMD). The left plot contains all stars detected in all 3 wavebands within $r \leq 33''$ (1 pc). Since NGC 3603 is located in the Galactic Plane we expect a significant contamination from field stars. To reduce this contribution we followed a statistical approach by subtracting the average number of field stars found in the regions around the cluster at $r \geq 75''$ (central plot) per magnitude and per colour bin (0.5 mag each). The accuracy of our statistical subtraction is mainly limited by three factors: first,

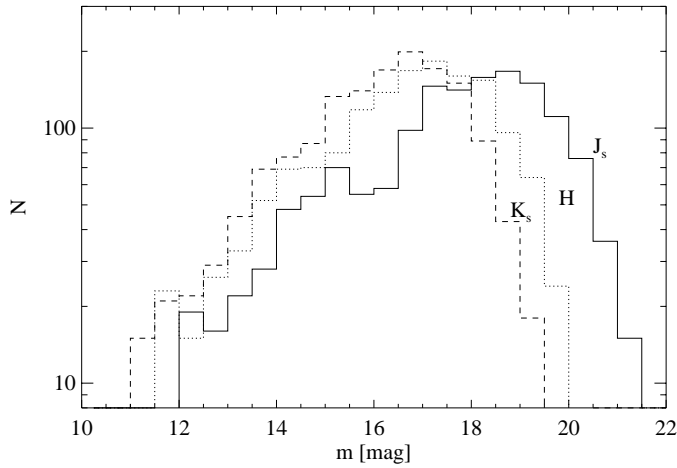


Fig. 3. The observed luminosity functions of stars detected at all 3 wavebands in the central stellar cluster with $r \leq 33''$ (1 pc). The magnitudes are apparent J_s (solid), H (dotted), and K_s (dashed) magnitudes. The number counts have not been corrected for incompleteness.

we cannot rule out that low-mass pre-main sequence stars are also present in the outskirts of the cluster. Second, because of crowding on one hand and dithering which leads to shorter effective integration times outside the central $2'.5 \times 2'.5$ on the other hand, the completeness limit varies across the FOV. Third, local nebulosities may hide background field stars. However, none of these potential errors affects our conclusions drawn from the CMD.

The resulting net CMD for cluster stars within $r \leq 33''$ of NGC 3603 is shown at the right in Fig. 2. We overlaid the theoretical isochrones of pre-main sequence stars from Palla & Stahler (1999) down to $0.1M_{\odot}$. We assumed a distance modulus of $(m - M)_{\odot} = 13.9$ based on the distance of 6 kpc (De Pree et al. 1999) and an average foreground extinction of $A_V = 4.5^m$ following the reddening law by Rieke & Lebofski (1985). Applying the isochrones to measured magnitudes could be misleading since the theoretical calculations include only stellar photospheres while the stars still may be surrounded by dust envelopes and accretion disks. This would lead to excess emission in the NIR and make the stars appear younger than they actually are. Typical excess emission of classical T Tauri stars in the Taurus–Auriga complex have been determined as $\Delta H = 0.2^m$, and $\Delta K = 0.5^m$ (Meyer, Calvet & Hillenbrand 1997). The upper part of the cluster-minus-field CMD clearly shows a main sequence with a marked knee indicating the transition to pre-main sequence stars. The turn-on occurs at $J_s \approx 15.5^m$ ($m \approx 2.9M_{\odot}$). Below the turn-on the main-sequence basically disappears. We note that the width of the pre-main sequence in the right part of Fig. 2 does not significantly broaden toward fainter magnitudes, indicating that our photometry is not limited by photometric errors. The scatter may in fact be real and due to varying foreground extinction,

infrared excess and evolutionary stage. In that case the left rim of the distribution would be representative of the “true” colour of the most evolved stars while the horizontal scatter would be primarily caused by accretion disks of different inclinations and ages. Fitting isochrones to the left rim in the CMD yields an age of only 0.3–1.0 Myr. Our result is in good agreement with the study by Eisenhauer et al. (1998) but extends the investigated mass range by about one order of magnitude toward smaller masses. Because of ≈ 10 magnitudes range in luminosities in the crowded core region our sensitivity limits of $J_s \approx 21^m$, $H \approx 20^m$ and $K_s \approx 19^m$ don’t appear to be exceedingly faint (and are about 3 magnitudes above ISAAC’s detection limit for isolated sources). However, only VLT/ISAAC’s high angular resolution, PSF stability, and overall sensitivity enabled us to study the sub-solar stellar population in a starburst region on a star by star basis.

Fig. 3 shows the luminosity functions for stars detected in all 3 wavebands. For the purpose of this letter we have not attempted to correct our number counts for incompleteness, i.e., an increasingly significant percentage of stars will be undetected toward fainter magnitudes. Thus we have no means to determine whether the apparent turnover at $K_s \approx 16.5^m$ is real or an observational artifact, but we do note that the mass spectrum is well populated down to $K_s \sim 19^m$, corresponding to a $0.1M_{\odot}$ pre-main sequence star of 0.7 Myr (Zinnecker, McCaughrean & Wilking 1993). A detailed analysis of the low-mass IMF will be the subject of a subsequent paper.

Acknowledgements. We would like to thank the ESO staff for their excellent work.

References

- Brandl, B., et al. 1996, ApJ, 466, 254
- Brandl, B., Brandner, W. & Zinnecker, H. 1999, Star Formation 1999, eds. T. Nakamoto et al., in press
- Brandner, W., et al. 1997, ApJ, 489, L153
- Brandner, W., et al. 2000, AJ, in press
- De Pree, C.G., Nysewander, M.C. & Goss, W.M. 1999, AJ, 117, 2902
- Drissen, L., Moffat, A.F.J., Walborn, N. & Shara, M.M. 1995, AJ, 110, 2235
- Eisenhauer, F., Quirrenbach, A., Zinnecker, H. & Genzel, R. 1998, ApJ, 498, 278
- Frogel, J.A., Persson, S.E., Aaronson, M. 1977, ApJ, 213, 723
- Hunt, L.K., et al. 1998, AJ, 115, 2594
- Kennicutt, R.C. Jr. 1984, ApJ, 287, 116
- Meyer, M.R., Calvet, N., & Hillenbrand, L.A. 1997, AJ, 114, 288
- Moffat, A.F.J., Drissen, L., & Shara, M.M. 1994, ApJ, 436, 183
- Palla, F. & Stahler, S.W. 1999, ApJ, in press (20 Nov)
- Persson, S.E. et al. 1998, AJ, 116, 247
- Rieke, G.H. & Lebofsky, M.J. 1985, ApJ, 288, 618
- Stetson, P.B. 1987, PASP, 99, 191
- Zinnecker, McCaughrean & Wilking 1993, Protostars and Planets III, eds. E.H. Levy & J.I. Lunine (University of Arizona Press), 429